

RESEARCH ARTICLE

The CELF1 RNA-Binding Protein Regulates Decay of Signal Recognition Particle mRNAs and Limits Secretion in Mouse Myoblasts

Joseph Russo¹, Jerome E. Lee^{1,2^{aa}}, Carolina M. López¹, John Anderson¹, Thuy-mi P. Nguyen^{1^{ab}}, Adam M. Heck^{1,2}, Jeffrey Wilusz^{1,2}, Carol J. Wilusz^{1,2*}

1 Department of Microbiology, Immunology and Pathology, Colorado State University, Fort Collins, Colorado, United States of America, **2** Program in Cell and Molecular Biology, Colorado State University, Fort Collins, Colorado, United States of America

^{aa} Current Address: ArcherDX, Boulder, Colorado, United States of America

^{ab} Current Address: Department of Laboratory Medicine and Pathology, Mayo Clinic, Rochester, Minnesota, United States of America

* cwilusz@colostate.edu



OPEN ACCESS

Citation: Russo J, Lee JE, López CM, Anderson J, Nguyen T-mP, Heck AM, et al. (2017) The CELF1 RNA-Binding Protein Regulates Decay of Signal Recognition Particle mRNAs and Limits Secretion in Mouse Myoblasts. PLoS ONE 12(1): e0170680. doi:10.1371/journal.pone.0170680

Editor: Yoon Ki Kim, Korea University, REPUBLIC OF KOREA

Received: August 19, 2016

Accepted: January 9, 2017

Published: January 27, 2017

Copyright: © 2017 Russo et al. This is an open access article distributed under the terms of the [Creative Commons Attribution License](https://creativecommons.org/licenses/by/4.0/), which permits unrestricted use, distribution, and reproduction in any medium, provided the original author and source are credited.

Data Availability Statement: All relevant data are within the paper and its Supporting Information files.

Funding: This work was supported by the National Institutes of Health (www.niams.nih.gov) through an award to CJW (AR059247) and by the National Science Foundation (www.nsf.gov) through an award to CJW and JW (MCB-1301983). JEL was supported in part by a pre-doctoral fellowship from the American Heart Association (www.heart.org; 10PRE2610140). AH was supported in part

Abstract

We previously identified several mRNAs encoding components of the secretory pathway, including signal recognition particle (SRP) subunit mRNAs, among transcripts associated with the RNA-binding protein CELF1. Through immunoprecipitation of RNAs crosslinked to CELF1 in myoblasts and *in vitro* binding assays using recombinant CELF1, we now provide evidence that CELF1 directly binds the mRNAs encoding each of the subunits of the SRP. Furthermore, we determined the half-lives of the *Srp* transcripts in control and CELF1 knockdown myoblasts. Our results indicate CELF1 is a destabilizer of at least five of the six *Srp* transcripts and that the relative abundance of the SRP proteins is out of balance when CELF1 is depleted. CELF1 knockdown myoblasts exhibit altered secretion of a luciferase reporter protein and are impaired in their ability to migrate and close a wound, consistent with a defect in the secreted extracellular matrix. Importantly, similar defects in wound healing are observed when SRP subunit imbalance is induced by over-expression of SRP68. Our studies support the existence of an RNA regulon containing *Srp* mRNAs that is controlled by CELF1. One implication is that altered function of CELF1 in myotonic dystrophy may contribute to changes in the extracellular matrix of affected muscle through defects in secretion.

Introduction

The concept of RNA regulons, in which functionally related genes are co-regulated by specific RNA-binding proteins (RBPs), was first proposed by Keene and Tenenbaum in 2002 [1]. Since that time, the advent of RNA immunoprecipitation-based high throughput approaches including CLIP-seq [2] and PAR-CLIP [3] has facilitated the identification of large datasets of mRNA targets for a variety of RBPs, including CELF1 [4–8]. Additional studies have indicated

through National Science Foundation -NRT Award # 1450032 to Thomas Chen, Carol Wilusz & Asa Ben-Hur. The funders had no role in study design, data collection and analysis, decision to publish, or preparation of the manuscript.

Competing Interests: The authors have declared that no competing interests exist.

that subcellular clustering of functionally related mRNAs through their interactions with RNA-binding proteins can result in a high local concentration of protein subunits to facilitate efficient macromolecular complex assembly [9]. Based on these ideas, altered function of a single RBP could have profound effects on the assembly/abundance of an entire multi-protein complex. Such regulation could be central to normal cellular responses, but might also be detrimental if the RBP were mutated or impaired by disease.

CELFI (CUG-binding protein, ELAV-Like Family member 1) is an RBP which regulates gene expression at multiple steps, including splicing, polyadenylation, translation and/or mRNA decay [10,11]. CELFI appears to be particularly important for skeletal muscle function as its over-expression in mice inhibits myogenesis [12], decreases muscular mass and function, and induces an array of muscular histological abnormalities [13]. Furthermore, several inherited human diseases affecting muscle display aberrant CELFI expression or localization [14–16]. In the best studied example, Type 1 Myotonic Dystrophy (DM1), CELFI is hyper-phosphorylated and over-expressed [14,17]. CELFI over-expression in DM1 has been connected with pathogenic splicing abnormalities [18–21], but its impact on other steps of mRNA metabolism such as decay and translation is less understood.

We chose to focus here on a putative RNA regulon containing six mRNAs encoding protein subunits of the signal recognition particle (SRP) [22]. The SRP is a cytoplasmic ribonucleoprotein complex composed of the 7SL structural RNA and six different protein subunits (SRP9, SRP14, SRP19, SRP54, SRP68 and SRP72) [22]. The vast majority of SRP biogenesis occurs in the nucleolus, before export to the cytoplasm where the final subunit, SRP54, is incorporated [23,24]. The SRP binds the signal peptide in nascent secreted and membrane-bound proteins and induces translational stalling [25]. When SRP associates with its receptor in the endoplasmic reticulum (ER), translation resumes and the nascent protein is translocated into the ER lumen. We selected the SRP transcripts for further study because coordinated expression of SRP mRNAs might be necessary for efficient SRP complex assembly. Moreover, the secretory pathway is essential for formation of a functional extracellular matrix (ECM), and ECM components are frequently mutated/disrupted in muscular dystrophies [26]. In addition, autoantibodies to SRP subunits are a primary cause of inflammatory myositis [27]; a condition that can be difficult to distinguish from muscular dystrophy [28].

In this study, we investigated the effects of CELFI expression on accumulation and decay of mRNAs encoding the SRP proteins, which we previously identified through RNA-immunoprecipitation [4]. We observed significant changes in the stability of *Srp* transcripts in response to CELFI knockdown. This is likely directly due to loss of CELFI as multiple experiments support direct binding of CELFI to *Srp* transcript 3'UTRs. Furthermore, SRP19 and SRP68 proteins are over-expressed following CELFI depletion. Our data support that this is sufficient to influence cellular processes dependent on the SRP as CELFI depletion and SRP68 over-expression can each cause defects in cell migration, which relies on secretion of the ECM.

Materials and Methods

Cell culture and transfections

C2C12 cells (ATCC CRL1772) were grown at 37°C, 5% CO₂ at or below 70% confluency in Dulbecco's Modified Eagle's Media (DMEM) containing 10% fetal bovine serum (FBS), penicillin (10 units/ml) and streptomycin (10 µg/ml). To create knockdown cell lines C2C12 myoblasts were infected using either a control lentivirus (LKO1) or a lentivirus encoding an shRNA against CELFI (sh1739 Sigma MISSION ID clone NM_198683.1-1739s1c1), pools of cells were selected with puromycin (4 µg/ml) and CELFI knockdown was then verified by

western blot [29]. CELFI expression was routinely reduced to less than 10% of control [4]. After the initial selection the stable cell lines were maintained in 1–2 $\mu\text{g/ml}$ puromycin.

Western blot analyses

30–50 μg of whole protein extract prepared by lysis of cells in RIPA buffer (50 mM Tris-Cl pH7.4, 150 mM NaCl, 0.5% deoxycholic acid, 1% NP-40, 1 mM EDTA, 0.05% SDS) were separated on 10% or 15% SDS-polyacrylamide gels and blotted onto polyvinylidene difluoride (PVDF) membrane. Suppliers, catalog numbers and concentrations for primary antibodies can be found in Table A in [S1 File](#). In all cases, anti-mouse or anti-rabbit horseradish peroxidase-conjugated secondary antibodies (Santa Cruz Biotechnology) were employed as appropriate, and detection was by the SuperSignal Pico West kit (Pierce) using a Bio-Rad ChemiDoc imager and the ImageLab software for quantification.

Gel shift analyses

Recombinant human GST-CELFI protein was purified from *E.coli* as previously described [30]. $\alpha^{32}\text{P}$ -UTP labeled transcripts were produced by *in vitro* transcription using SP6 or T7 RNA polymerase. Templates for transcription were obtained by PCR from murine cDNA with primers specified in Table B in [S1 File](#). Each template contained the region indicated flanking the putative GU-rich CELFI binding sites. The negative control template was a transcript derived from the 7SL RNA which does not contain CELFI-binding sites. Increasing concentrations of GST-hCELFI protein were incubated with 3 fmol of RNA transcript and separated on a 5% native polyacrylamide gel as described previously [31].

Formaldehyde cross-linking and RNA immunoprecipitation

RNA immunoprecipitation experiments were performed after formaldehyde cross-linking of myoblasts using a procedure based on that described previously [32]. Briefly, C2C12 cells were grown to ~60% confluency and cross-linking of RNA complexes was achieved by incubating the cells for 10 minutes in 1 X Phosphate Buffered Saline (PBS) containing 1% formaldehyde. Glycine (pH 7.0) was added to a final concentration of 250 mM and cells were rocked for 5 minutes to quench the reaction. Cells were washed three times in PBS and harvested by centrifugation. Cell pellets were resuspended in an equal volume of RIPA buffer and lysed by sonication. The RNA-CELFI complexes were immunoprecipitated from cleared whole cell lysates by incubating with 2 μg of anti-CELFI antibody (mAb 3B1; Santa Cruz Biotechnologies) or normal mouse IgG antibody on ice for 1 hour. Protein-G sepharose resin was added to precipitate bound complexes. Precipitates were washed twice each in NT2 (50 mM Tris-Cl pH 7.4, 150 mM NaCl, 1 mM MgCl_2 , 0.05% Nonidet P-40), RIPA, and High-Stringency RIPA (50 mM Tris-Cl pH 7.4, 1% NP-40, 0.1% Sodium Deoxycholate, 0.1% SDS, 1 mM EDTA, 1M NaCl, 1 M Urea, and 0.2 mM PMSF), for 10 minutes each. Crosslinks were reversed by incubation in crosslink reversal buffer (50 mM Tris-Cl pH 7.0, 0.5 mM EDTA, 10 mM DTT, and 1% SDS) for 40 minutes at 70°C. The RNA was isolated using TRIzol[®] (ThermoFisher) extraction according to the manufacturer's recommendations. cDNA was synthesized using random hexamers and Improm II Reverse Transcriptase (Promega) and subsequently used for PCR with primers specific for the 3' UTR of the *Srp* mRNAs or for *Myc* mRNA as a negative control (see Table B in [S1 File](#)).

Luciferase secretion assays

Control and CELFI KD myoblasts were transfected using Lipofectamine[™] 2000 (Life Technologies) [31] in a 96-well plate format with two reporter plasmids; one encoding a Firefly

luciferase (FLuc; pLightSwitch_3'UTR from SwitchGear Genomics) and the other encoding a Gaussia luciferase (GLuc) bearing an N-terminal signal peptide [33]. Approximately 18 hr post-transfection, activity of the secreted GLuc in the media was measured by addition of the coelenterazine substrate (Nanolight Technology). Also, to account for variation in transfection efficiency, the FLuc activity in the cells was measured using the Steady Glo reagent (Promega). The signal from each luciferase was read in a Victor plate reader (Perkin Elmer). The GLuc reading was normalized to that of FLuc in each experiment.

Analysis of mRNA abundance and half-lives

mRNA half-lives were determined as described previously [34] but using MTSEA-Biotin-XX rather than HPDP-biotin for conjugation [35]. Control (LKO1) and CELFI KD cells were grown to ~60% confluency then incubated in 400 μ M 4-thiouridine (4sU; SIGMA). After 12 hours, total RNA was extracted via TRIzol[®] (ThermoFisher) and treated with DNase I. Total RNA was subjected to biotinylation as follows: 20–40 μ g of total RNA was spiked with total RNA extracted from *S. cerevisiae* that had been treated with 5mM 4-thiouracil for 5 min (see [36] for details) at a ratio of 5 μ g C2C12 RNA to 1 μ g of yeast RNA. The yeast RNA acted as an internal control for the biotinylation and fractionation process. Biotinylation was performed as described [35]. Briefly, 15 μ L of 10X biotinylation buffer (100mM HEPES [pH 7.5], 10mM EDTA) and 10 μ L 1mg/mL MTSEA-biotin-XX (Biotium) in 20% dimethylformamide were added to the RNA in a final volume of 150 μ L and incubated in the dark at room temperature with gentle agitation for 2 hours. After incubation, excess MTSEA-biotin-XX was removed by chloroform/isoamylalcohol extraction using Phase-Lock Gel Heavy 1.5mL tubes (5 PRIME). The RNA was precipitated and reconstituted in 105 μ L of ddH₂O. The RNA was fractionated as follows: 50 μ L of RNA was bound to μ MACS Streptavidin Microbeads (Miltenyi Biotech). Following two washes with high salt wash buffer (100 mM Tris-HCl (pH7.4), 10 mM EDTA, 1M NaCl and 0.1% Tween-20) the nascent (4sU-labeled) RNA was eluted from the column with 100mM DTT. All three fractions (Total, Flow-through/Pre-Existing and Nascent) were precipitated in the presence of glycogen, washed and resuspended in an equal volume of ddH₂O. 1 μ L of total and nascent RNA were used to make cDNA using random hexamers and Improm II reverse transcriptase (Promega). Digital PCR (dPCR) was performed using primers specific to each SRP gene as well as yeast MFA2 as a control for biotinylation and fractionation using QX200 ddPCR EvaGreen supermix (Bio-Rad) according to the manufacturer's recommendations. Total and nascent RNA copy numbers were normalized to the recovery for each sample (as determined by yeast MFA2 mRNA nascent/total ratio) to acquire abundances. Half-lives were determined using the equation $t_{1/2} = t_L \times \ln(2)/\ln(1-R)$, where t_L = labeling time and R = abundance in nascent RNA fraction/abundance in total RNA fraction. Labeling and fractionation were performed in triplicate, average half-lives were determined along with the standard error of the mean (SEM). A paired t-test (two-tailed) was performed to determine statistical significance. Abundances of *Srp* mRNAs were determined from the abundance in the total RNA fraction and normalized to levels of *Rumx3* mRNA which was selected as an appropriate reference gene based on expression level and lack of variation between the Control and CELFI KD cell lines. A paired t-test was used to determine statistical significance. Primers are described in Table B in S1 File. All primer sets were verified to perform with efficiencies of 90–110% and to generate a single product of the expected molecular weight.

Over-expression of SRP68

The entire open reading frame of the murine SRP68 gene (*NM_146032.3*) was amplified by PCR using cDNA derived from C2C12 cells as a template. The resulting PCR product was

digested with *EcoRI* and *BamHI* and cloned into the p3xFlag-CMV10 expression vector (Sigma). The primer sequences are shown in Table B in [S1 File](#). The resulting construct or the empty vector were transfected into C2C12 cells as described above [31] and increased expression of SRP68 was verified by western blot 24 hrs later.

Wound healing assays

These were performed essentially as described previously [37]. Equal numbers of control and CELFI KD C2C12 myoblasts or control and SRP68 over-expressing myoblasts were allowed to reach near confluency in growth media. The tip of a pipette was used to scratch and remove the monolayer. The cells were washed twice with PBS buffer which was replaced with pre-warmed DMEM containing 0.1% FBS to minimize proliferation. The wound was imaged at 10X magnification. After incubation the cells were washed in PBS and reimaged. The number of cells that had migrated into the wound area was counted and the number in CELFI KD or SRP68 over-expressing cells is represented as a percentage of those migrating in the control cells.

Results

CELFI associates with Srp mRNAs

We previously used RNA-immunoprecipitation followed by microarray (RIP-Chip) to identify mRNAs associated with CELFI [4]. Amongst the top 5% most enriched transcripts were several mRNAs encoding factors belonging to the secretory pathway, including three of the six protein subunits of the Signal Recognition Particle (*Srp54*, *Srp72* and *Srp68*). A more relaxed analysis (top 10% most enriched) suggested that *Srp9* and *Srp19* mRNAs were also significantly enriched in the CELFI immunoprecipitate. In support of this, CELFI CLIP-seq performed by others using mouse C2C12 cells identified binding sites in the 3'UTRs of *Srp9*, *Srp14* and *Srp72* mRNAs [5]. Both RIP-Chip and CLIP-seq have been used to identify RNA targets bound by CELFI in HeLa cells and these also pinpointed *Srp* mRNAs as targets of CELFI [8,38]. Thus multiple independent studies support that CELFI binds to *Srp* mRNAs in human and mouse.

Based on these observations, we hypothesized that CELFI might play a role in coordinating expression of the SRP subunits to facilitate optimal assembly of the SRP complex. CELFI binding through the 3'UTR can influence polyadenylation [39], translation [40,41], decay [11] and/or localization [42] of mRNAs, any of which could influence overall protein levels. We found GU-rich sequences resembling CELFI binding sites in the 3'UTRs of all the *Srp* mRNAs (Table 1) supporting that the 3'UTR is the most likely binding site. In order to confirm this, we performed electrophoretic mobility shift assays, using recombinant human CELFI protein and *in vitro* transcribed RNA fragments containing putative CELFI binding site(s) derived from each of the *Srp* 3'UTRs. We found that all the 3'UTR fragments bound the recombinant protein with affinities ranging from 0.53 to 33.8 nM (Table 1 and Fig 1). In contrast, a fragment of the 7SL RNA, which contains no identifiable CELFI binding sites, was not appreciably bound by CELFI under the conditions employed ($K_d > 300$ nM (Fig 1)). We conclude that CELFI is capable of binding the 3' UTRs of all *Srp* mRNAs with high affinity *in vitro*. We cannot however rule out that CELFI binds these mRNAs in additional locations *in vivo* as the complete 3'UTRs containing all possible binding sites were not tested, primarily due to limitations in separating protein complexes containing larger RNA fragments.

The *in vitro* results were not entirely consistent with those obtained in our RIP-Chip experiment in that CELFI appears to recognize the *Srp14* 3'UTR in our gel shift assays but this transcript was not enriched in the CELFI immunoprecipitate. One possible explanation is that the interaction was lost during the immunoprecipitation. We therefore repeated the RNA

Table 1. CELF1 binding to 3'UTR of *Srp* mRNAs *in vitro*.

Gene	3'UTR length (nt)	Putative CELF1 binding sites			K _d (nM)
<i>Srp9</i>	960	GUGUUUUUUGUA	GUGUUGUC		0.84 ± 0.12
<i>Srp14</i>	380	UUUGUUU			12.4 ± 1.8
<i>Srp19</i>	371	UUUGUUUGUC			33.8 ± 1.7
<i>Srp54</i>	2475	UUUGUGUUUUUGU	AGGUGUUUUUCUG		13.5 ± 1.0
<i>Srp68</i>	536	UUUGUGUUUUUGUC	GUGUUUGUC	CUGUGUC	1.64 ± 0.29
<i>Srp72</i>	1566	GUGUGUGUGUAUUUGUC	UGUACCUUUUGUUUUUC		0.53 ± 0.08

GU-rich regions contained within each fragment that could act as CELF1 binding sites are shown. 3'UTR fragments ranging from 120–264 nt in length containing GU-rich elements were used for electrophoretic mobility shifts to derive the dissociation constants. Errors are standard deviations from three independent replicates.

doi:10.1371/journal.pone.0170680.t001

immunoprecipitation but this time using protein extracts from cells that had been cross-linked with formaldehyde prior to cell lysis to stabilize protein/RNA interactions during the isolation and immunoprecipitation. A control immunoprecipitation using normal IgG was also performed in parallel. RT-PCR was then used to detect CELF1-associated transcripts in the immunoprecipitate. As shown in Fig 2, all six *Srp* transcripts were readily detected in the anti-CELF1 immunoprecipitate but not in the control IgG immunoprecipitate. As expected, a control transcript that does not contain GU-rich elements, *Myc*, was not associated with CELF1. These results demonstrate that CELF1 can associate with all the *Srp* mRNAs in living cells, but binding to *Srp14* mRNA may be more easily disrupted than the other associations as it was not observed without cross-linking [4].

CELF1 depletion stabilizes *Srp* mRNAs

We next wanted to determine the consequences of CELF1 binding on *Srp* mRNA decay. We were able to use data generated from our previous global analysis of mRNA decay rates in C2C12 cells [4] to estimate the normal half-lives for each of the *Srp* mRNAs. The calculated mRNA half-lives ranged from 2.7 hr for *Srp68* to almost 6 hr for *Srp72* (Fig A in S1 File). The standard approach to assay mRNA decay rates, used in our previous study, involves inhibition of transcription with Actinomycin D (ActD). This method is less than ideal when assaying relatively stable mRNAs due to the toxicity of prolonged treatment [43,44]. Therefore, we adopted an assay based on the incorporation of 4-thiouridine (4sU) into nascent transcripts, which has fewer and less drastic effects on cell health [34,35]. Briefly, Control and CELF1 KD cells were treated with 4sU for 12 hours and total RNA isolated. Upon addition of 4sU (t = 0 min), unlabeled transcripts cease to accumulate and the change in their abundance at subsequent time points reflects their rate of decay. The newly synthesized 4sU-containing transcripts were conjugated to biotin and enriched by passing over streptavidin-agarose. We measured the abundance of each *Srp* mRNA in total RNA before fractionation and in the labeled fraction using the ratio to derive a half-life for each transcript (see Materials & Methods for equation and additional details). In control cells, the half-lives for all the transcripts, except *Srp72*, were longer than those derived using ActD treatment (Fig B in S1 File) supporting the notion that ActD has unwanted and unpredictable effects on mRNA decay [45,46]. *Srp19*, *Srp54*, *Srp68* and *Srp72* all had half-lives in a similar range (3.3–7.8 hr) while *Srp9* and *Srp14* were considerably more stable (17.4 and 13.5 hr respectively) (Fig 3A and Fig B in S1 File). These half-lives were similar to those derived by 4sU labeling in murine NIH 3T3 fibroblasts [47], except for *Srp9* which appears significantly more stable in C2C12 cells than in fibroblasts (Fig B in S1 File).

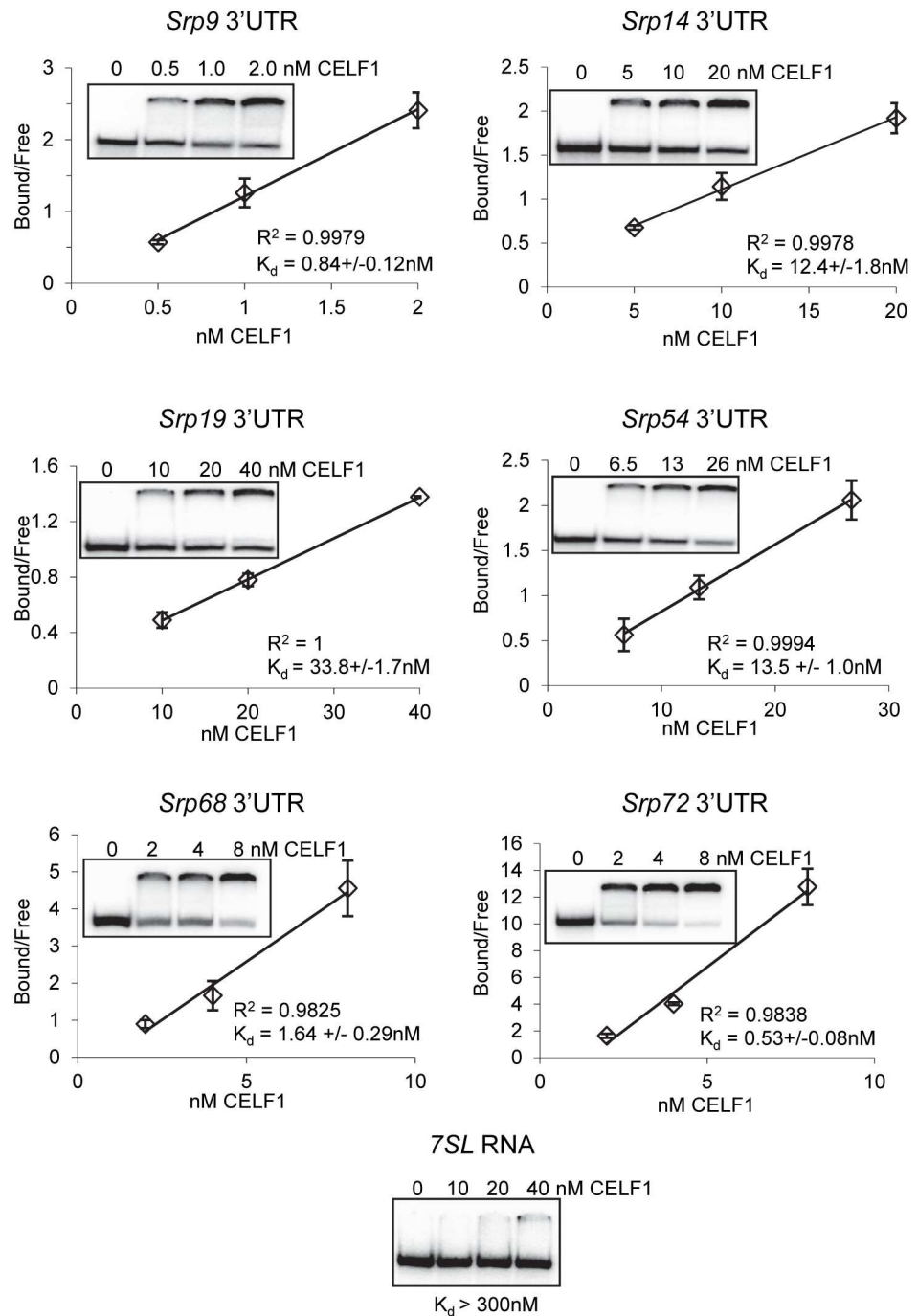


Fig 1. Sequence elements derived from the 3'UTRs of SRP mRNAs are bound by CELF1. Increasing concentrations of recombinant CELF1 were incubated with radio-labeled RNA fragments and separated on a native acrylamide gel. The proportion of RNA that bound to CELF1 was used to derive a dissociation constant.

doi:10.1371/journal.pone.0170680.g001

When we compared the half-lives in the control cells to those in the CELF1 KD myoblasts, we found that all transcripts except for *Srp68* mRNA showed significant increases in half-life in the CELF1 KD cells (Fig 3A). As shown in Fig 3B, both the mean half-life and the range of half-lives for all *Srp* mRNAs are greater in the CELF1 KD cells than in the controls. At the

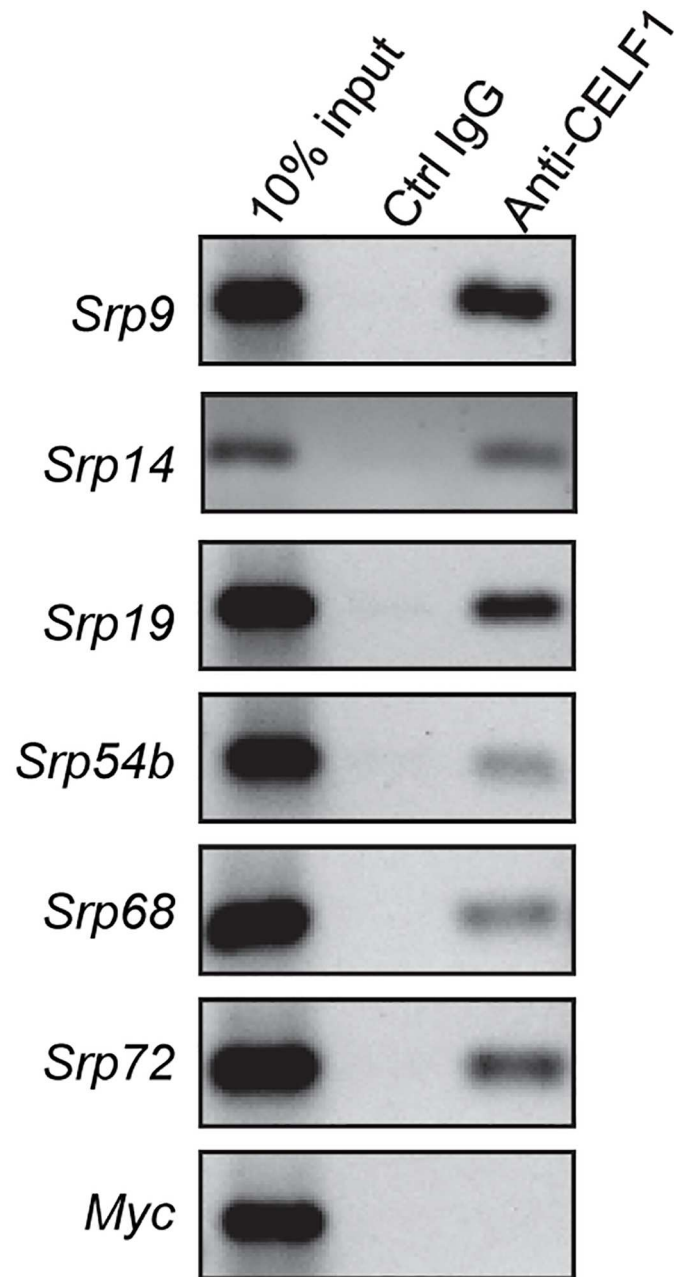


Fig 2. *Srp* mRNAs are associated with CELF1 in C2C12 myoblasts. C2C12 cells were treated with formaldehyde to stabilize protein-RNA interactions. Extracts were immunoprecipitated with anti-CELF1 antibody or a control IgG and Protein-G sepharose. RNAs associated with each immunoprecipitate were isolated and subject to reverse transcription and 35 or 42 (*myc*, *Srp14*) cycles of PCR. Products were separated on agarose gels and visualized by ethidium bromide staining.

doi:10.1371/journal.pone.0170680.g002

same time, we evaluated the decay of the RNA subunit of the SRP complex, 7SL RNA, which is not directly associated with CELF1. We found that the decay of 7SL RNA is not affected by CELF1 KD (Fig 3A).

We also examined the abundance of *Srp* mRNAs following CELF1 KD but did not see any dramatic differences (Fig 4A). On the surface this is surprising given that some of the

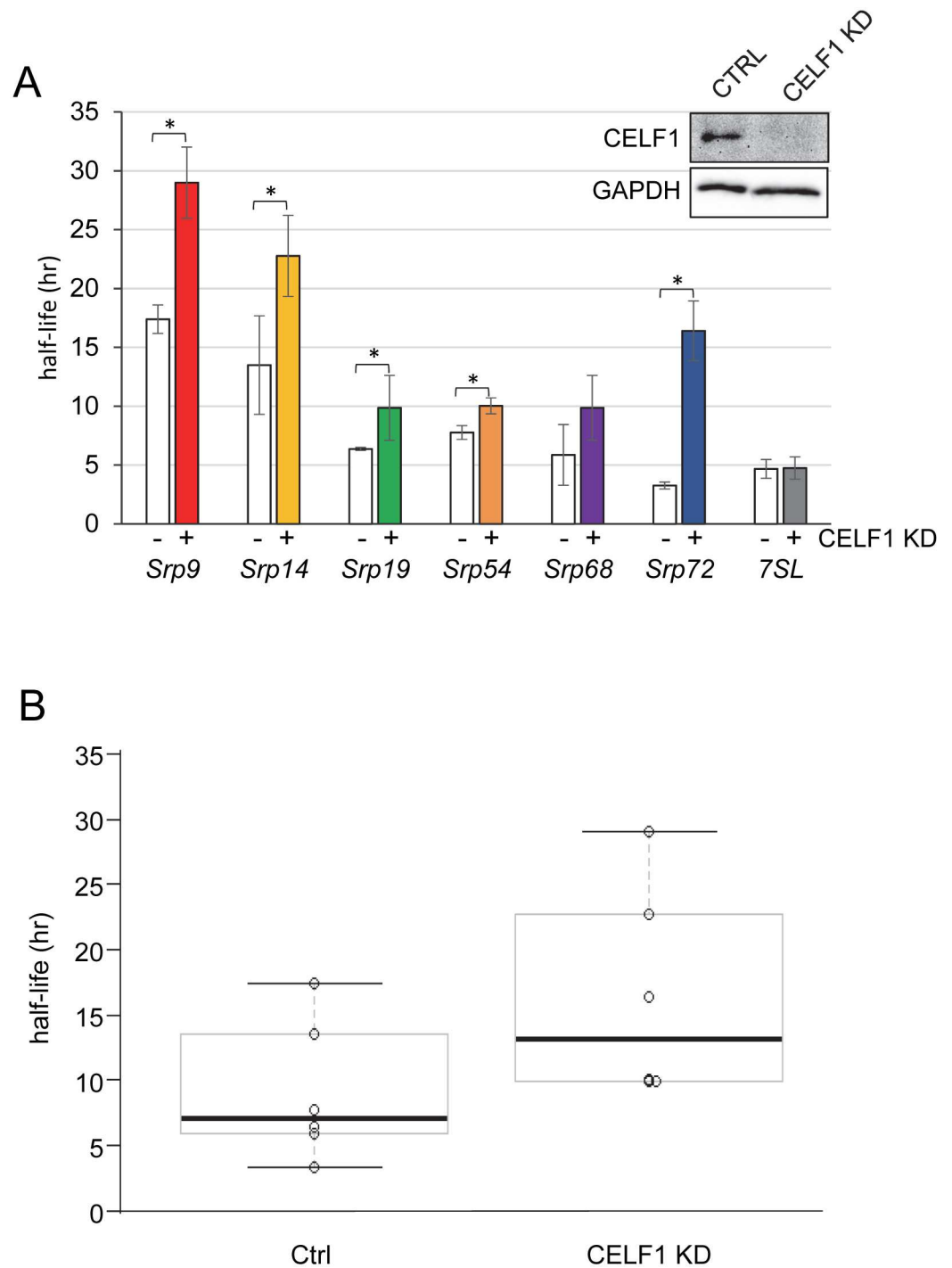


Fig 3. Srp mRNAs are stabilized following CELFI knockdown. A: Control (white bars) and CELFI KD (filled bars) C2C12 cells were treated with 4sU and total RNA was isolated at 12 hours. Following biotinylation and fractionation, the abundance of each *Srp* mRNA in total and labeled fractions was determined by dPCR and used to derive the half-life. The results were derived from three independent experiments for all except *Srp54* and 7SL RNAs which were derived from two experiments. The error bars represent the standard error of the mean. Asterisks denote $p < 0.05$. The inset shows a western blot verifying that CELFI protein was effectively undetectable in CELFI KD cells, GAPDH was evaluated as a loading control. B: *Srp* mRNA half-lives in Control and CELFI KD C2C12 cells derived from the graphs in (A) are plotted for comparison.

doi:10.1371/journal.pone.0170680.g003

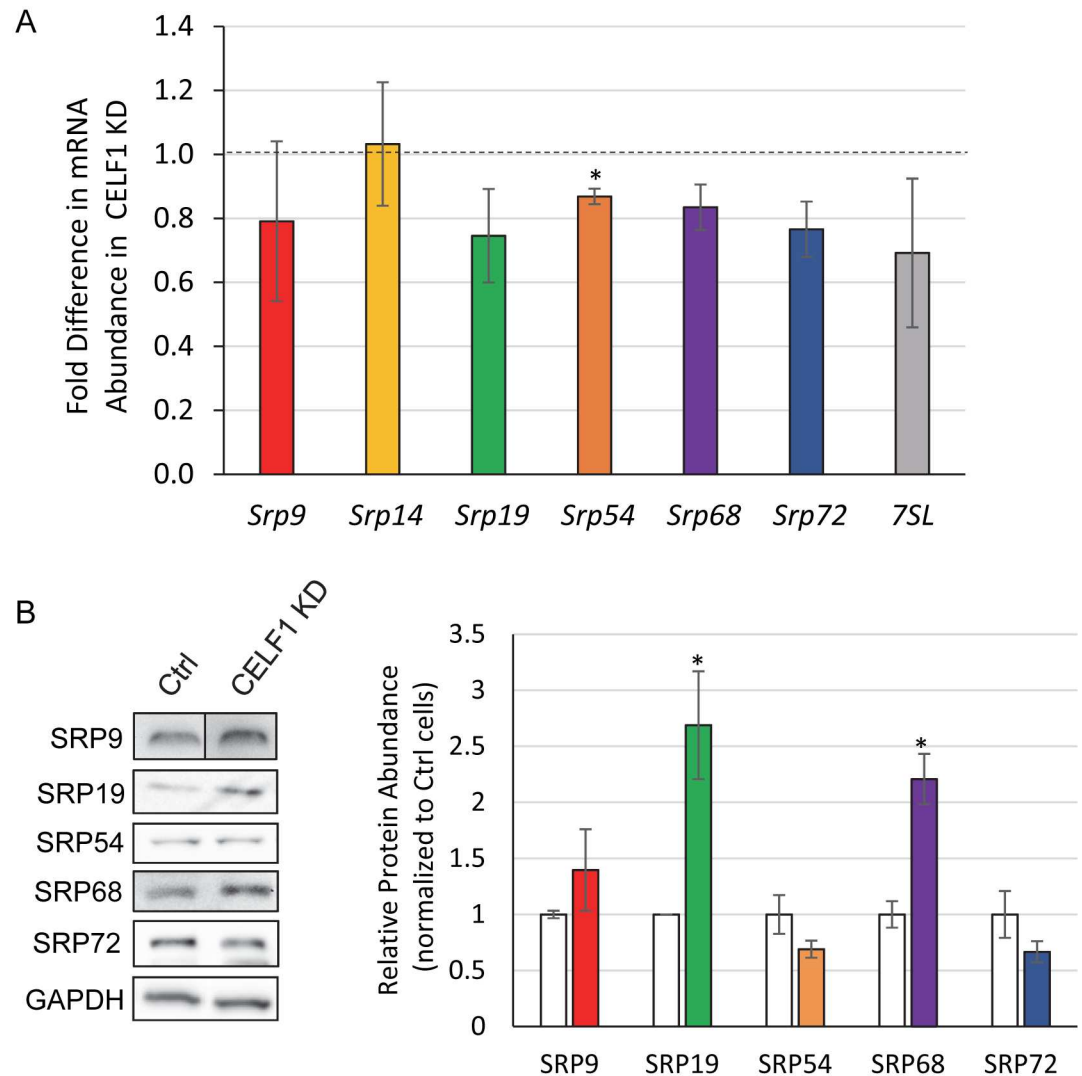


Fig 4. SRP protein expression is affected in CELFI KD cells. A: Abundance of *Srp* mRNAs was determined by dPCR and normalized to *Runx3* mRNA abundance. The fold change in abundance of each *Srp* RNA in CELFI KD cells is shown. Error bars represent the standard error of the mean for three independent replicates. Statistical significance was determined by paired t-test. The asterisk denotes $p < 0.05$. B: Abundance of SRP proteins in whole cell lysates from Control and CELFI KD cells was assessed by western blotting (left panel). For quantification, the abundance of GAPDH was used for normalization. In the graph, (right panel) SRP protein abundances in CELFI KD (colored bars) are shown relative to the abundance in the Control (Ctrl) cell line (white bars). Error bars represent the standard error of the mean derived from three independent experiments. Statistical significance was determined using the t-test. Asterisks indicate $p < 0.05$.

doi:10.1371/journal.pone.0170680.g004

transcripts show large changes in mRNA decay rate (Fig 3A). However, we and others have found that the effects of mRNA decay on abundance are not generally predictable [37,48,49]. This phenomenon has been attributed to the existence of poorly characterized buffering mechanisms that alter transcription rates to compensate for undesirable changes in mRNA decay [50–52] and to effects of RBP depletion on expression of transcription factors [48].

We next wanted to assess whether the effect of CELFI on *Srp* mRNA stability results in an effect at the protein level. We measured SRP protein levels by western blot in control and CELFI KD myoblasts and found the levels of SRP19 and SRP68 proteins were reproducibly

increased over two-fold in the CELFI KD cells (Fig 3B). The abundance of the other three SRP proteins that we were able to identify effectively for was not significantly altered. Therefore, the relative levels of the SRP subunits are out of balance in the CELFI KD cells, with SRP68 and SRP19 present in excess.

CELFI depletion results in enhanced protein secretion

Our results point to CELFI having an important role in regulating the overall abundance of the SRP subunits. We therefore examined whether there was an effect on the overall secretory capacity of cells depleted of CELFI using a *Gussia* luciferase (GLuc) that bears a signal peptide and is efficiently secreted into the media [33]. We transfected control and CELFI KD myoblasts with plasmids encoding the secreted GLuc and a cytoplasmic Firefly luciferase (FLuc). The next day, the media was assayed for GLuc activity and the cells were lysed and assayed for FLuc activity. GLuc activity was then normalized to FLuc to control for differences in transfection efficiency. We found GLuc was reproducibly secreted more efficiently in the CELFI KD cells (Fig 5A). Similar results were obtained in CELFI KD cells expressing an shRNA targeting a different region of the CELFI mRNA, verifying that the effect on secretion is specific to CELFI KD (data not shown).

CELFI depletion impairs wound healing

Production of the extracellular matrix (ECM) is exquisitely dependent on the secretory pathway [53]. We therefore hypothesized that cellular functions such as cell migration, which relies heavily upon the cell interactions with the ECM, might be affected in CELFI KD cells. We used a wound healing assay to investigate. Briefly, Control and CELFI KD cells were grown to near confluency and then scratched to remove the monolayer. The cells were incubated in low serum media to reduce proliferation and healing was assessed by counting the number of cells migrating into the wound after six hours. We observed that CELFI KD cells reproducibly performed poorly compared to controls in this assay (Fig 5B and 5C). This result is consistent with our finding of enhanced secretion in CELFI KD cells; alterations in the levels of secreted ECM proteins and membrane bound receptors are expected to modulate cell-matrix interactions that influence migration [54].

Over-expression of SRP68 impairs wound healing

If the defects in wound healing in CELFI knockdown cells are connected with SRP subunit imbalance, then increasing abundance of SRP subunits by other mechanisms should be sufficient to induce a similar phenotype. Indeed, when we transfected C2C12 cells with plasmid encoding Flag-SRP68 protein we were able to detect a reduction in cell migration (Fig 5D–5F) similar to that induced by CELFI depletion. This suggests that SRP68 may be a limiting factor in assembly of functional SRP.

Discussion

In this study, we demonstrated that the CELFI RNA-binding protein can specifically associate with sequences in the 3'UTR of each of the SRP mRNAs *in vitro* and in cultured myoblasts. Depletion of CELFI resulted in stabilization of five SRP mRNAs and increased abundance of SRP19 and SRP68 proteins. Depletion of CELFI also induced phenotypes consistent with disruption of the secretory pathway: CELFI KD cells exhibited an increased ability to secrete a luciferase protein and slower migration in a wound healing assay. Finally, the defects in cell

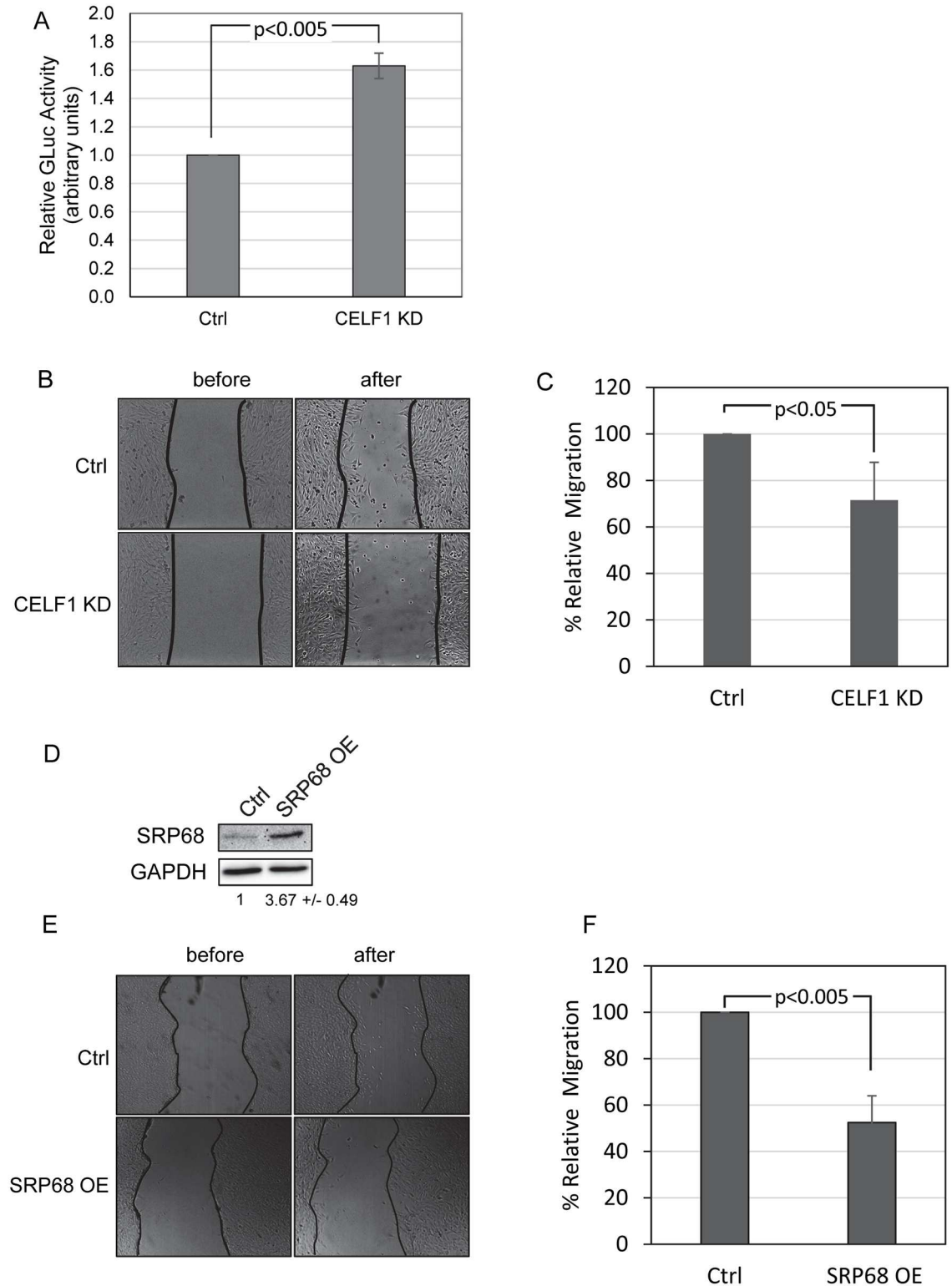


Fig 5. CELF1 KD cells have increased secretory capacity and perform poorly in wound healing assays. A: Control (Ctrl) and CELF1 KD cells were co-transfected with constructs encoding secreted and cytoplasmic luciferase proteins. Gaussia luciferase activity in the media was normalized to cytoplasmic firefly luciferase activity. Errors represent the standard deviation from three independent experiments. B: Control (Ctrl) and CELF1 KD cells were grown to ~90% confluence and then displaced by scratching. The cells were imaged immediately and again after incubation. C: The

number of cells migrating into the wound is represented as a percentage of the number in the control cells. The error bars represent the standard deviation from three experiments. D: Western blot demonstrating that SRP68 is over-expressed following transfection of a construct encoding the murine SRP68 protein. E: Following transfection of the SRP68 over-expression construct or a control empty vector, wound healing assays were performed as described for B. F: Wound healing was quantified as for C.

doi:10.1371/journal.pone.0170680.g005

migration could be recapitulated by over-expression of SRP68, independent of CELFI knockdown.

Our results demonstrate that CELFI can bind to the 3'UTRs of all six SRP mRNAs, and influences the rate of decay for at least five SRP transcripts (*Srp9*, *Srp14*, *Srp19*, *Srp54* and *Srp72*) as well as the abundance of SRP19 and SRP68 proteins. Taken together, these data support that the SRP complex relies on CELFI to maintain an appropriate balance of the individual subunits, however the overall impact of CELFI binding may be different for each transcript. In part, this may reflect the affinity of CELFI for the 3'UTR of each transcript—CELFI had the highest affinity for the *Srp72* 3'UTR sequences (Table 1), and this mRNA was the most stabilized following loss of CELFI (Fig 2A). However, the position of the CELFI binding site with respect to other elements such as miRNA binding sites, binding sites for other RBPs may also play a role. For example, HuR and MBNL1 proteins are known to compete with CELFI for binding and regulation of some RNA substrates [7,40,41]. Such competition might mask the effects of CELFI knockdown under conditions where binding of another factor prevails.

Although we might have predicted that SRP subunits would have similar protein abundances in normal cells as they form a single complex, proteomics data from myotubes and skeletal muscle suggest that this may not in fact be the case (Fig C in S1 File [55]). It is possible that the more abundant subunits have other functions in addition to being components of the active SRP. For example, in human cells, SRP9 and SRP14 are present in excess and form a complex with the primate-specific Alu RNA [56]. In addition, fragments of 7SL RNA generated by Dicer cleavage may associate with a subset of SRP subunits and influence their association with the full length 7SL [57,58]. Alternatively, the limiting subunits may be upregulated under certain conditions to allow increased secretory capacity, or some subunits may be incorporated into the SRP less efficiently requiring that they be present at a higher concentration. At the protein level, we found that SRP19 and SRP68 were elevated following CELFI KD. If association of these two subunits were inefficient, then increasing their concentration could enhance complex assembly and increase the overall abundance of functional SRP. In support of this idea, we found that over-expression of SRP68 is sufficient to impair cell migration, consistent with an increase in secretion of ECM components.

Association of SRP mRNAs with CELFI potentially allows them to be regulated in a coordinated fashion by any stimuli that alter CELFI abundance or activity by influencing translation, turnover and/or post-translational modification of CELFI. To our knowledge, natural conditions that result in altered levels of SRP proteins have not been identified, but conditions that influence CELFI activity have been described. For example, during T cell activation, CELFI is phosphorylated leading to reduced binding to its targets [59]. The target RNA regulon in this case encodes proteins necessary for the transition out of quiescence and CELFI inactivation therefore allows rapid upregulation in response to extracellular signals. CELFI activity is also disrupted in DM1, where the protein is hyper-phosphorylated and over-expressed [17]. The precise effect on CELFI function and activity remains unclear, but evidence suggests that the splicing activity of CELFI is elevated in DM1 [7,13] supporting that in this case the protein can maintain its association with RNA. Thus in DM1 it is possible that over-expression of CELFI could destabilize target transcripts, including the *Srp* mRNAs.

We note that the stabilization of *Srp* mRNAs in CELF1 knockdown cells has little influence on the abundance of these mRNAs at steady state (Fig 4A). It is important to note that changes in mRNA stability have the biggest impact during a cellular response. More stable mRNAs take longer to reach a new steady state following induction or repression of transcription [60]. This means that the response to a stimulus will be slower. Thus, the biological impact of stabilizing CELF1-regulated mRNAs may be exacerbated under conditions where target transcripts are normally up- or down-regulated.

The association of CELF1 with mRNAs encoding components of the secretory pathway is intriguing, given that muscle is exquisitely dependent on secretion both for deposition of a functional extracellular matrix to transduce its contractile activity, and for myokine signaling. Moreover, defects in muscular ECM components are connected with various muscular dystrophies [26]. Our results show that knockdown of CELF1 enhances secretion of a reporter and slows migration in C2C12 cells. It seems possible therefore that the mis-regulation of CELF1 in DM1 may contribute to pathogenesis by disrupting secretion of ECM and/or other extracellular proteins resulting in a muscular dystrophy despite the fact that the gene affected in DM1, DMPK, does not encode an ECM component. Whether the secretion defect seen in CELF1 KD cells is directly connected to regulation of secretory pathway mRNAs or through another mechanism will require further investigation, but the fact that over-expressing SRP68 protein induces similar phenotypes is certainly consistent with this idea.

Supporting Information

S1 File. Supporting information. This file contains Fig A-C and Tables A and B as supporting information.
(PDF)

Acknowledgments

The digital PCR experiments were performed using instruments within the Molecular Quantification Core at Colorado State University. We thank Dr Bakhos Tannous for providing the Gluc plasmid. We are grateful to members of the Wilusz Lab for discussion.

Author Contributions

Conceptualization: CJW JW.

Formal analysis: AH JR JEL CML CJW JA.

Funding acquisition: CJW JW JEL.

Investigation: JR JEL CML JA TPN.

Methodology: CJW JEL JR CML JA.

Project administration: CJW.

Supervision: CJW JW.

Visualization: CJW AH JEL JR.

Writing – original draft: CJW.

Writing – review & editing: JW JR JA CML JEL TPN AH CJW.

References

1. Keene JD, Tenenbaum SA. Eukaryotic mRNPs may represent posttranscriptional operons. *Mol Cell*. 2002; 9: 1161–1167. PMID: [12086614](#)
2. Yeo GW, Coufal NG, Liang TY, Peng GE, Fu X-D, Gage FH. An RNA code for the FOX2 splicing regulator revealed by mapping RNA-protein interactions in stem cells. *Nat Struct Mol Biol*. 2009; 16: 130–137. doi: [10.1038/nsmb.1545](#) PMID: [19136955](#)
3. Hafner M, Landthaler M, Burger L, Khorshid M, Hausser J, Berninger P, et al. Transcriptome-wide identification of RNA-binding protein and microRNA target sites by PAR-CLIP. *Cell*. 2010; 141: 129–141. doi: [10.1016/j.cell.2010.03.009](#) PMID: [20371350](#)
4. Lee JE, Lee JY, Wilusz J, Tian B, Wilusz CJ. Systematic analysis of cis-elements in unstable mRNAs demonstrates that CUGBP1 is a key regulator of mRNA decay in muscle cells. *PLoS One*. 2010; 5: e11201. doi: [10.1371/journal.pone.0011201](#) PMID: [20574513](#)
5. Masuda A, Andersen HS, Doktor TK, Okamoto T, Ito M, Andresen BS, et al. CUGBP1 and MBNL1 preferentially bind to 3' UTRs and facilitate mRNA decay. *Sci Rep*. 2012; 2: 209. doi: [10.1038/srep00209](#) PMID: [22355723](#)
6. Vlasova-St Louis I, Bohjanen PR. Coordinate regulation of mRNA decay networks by GU-rich elements and CELF1. *Curr Opin Genet Dev*. 2011; 21: 444–451. doi: [10.1016/j.gde.2011.03.002](#) PMID: [21497082](#)
7. Wang ET, Ward AJ, Cherone JM, Giudice J, Wang TT, Treacy DJ, et al. Antagonistic regulation of mRNA expression and splicing by CELF and MBNL proteins. *Genome Res*. 2015; 25: 858–871. doi: [10.1101/gr.184390.114](#) PMID: [25883322](#)
8. Le Tonquèze O, Gschloessl B, Legagneux V, Paillard L, Audic Y. Identification of CELF1 RNA targets by CLIP-seq in human HeLa cells. *Genomics Data*. 2016; 8: 97–103. doi: [10.1016/j.gdata.2016.04.009](#) PMID: [27222809](#)
9. Nielsen FC, Hansen HT, Christiansen J. RNA assemblages orchestrate complex cellular processes. *BioEssays* 2016;
10. Dasgupta T, Ladd AN. The importance of CELF control: molecular and biological roles of the CUG-BP, Elav-like family of RNA-binding proteins. *Wiley Interdiscip Rev RNA*. 2012; 3: 104–121. doi: [10.1002/wrna.107](#) PMID: [22180311](#)
11. Vlasova-St Louis I, Dickson AM, Bohjanen PR, Wilusz CJ. CELFish ways to modulate mRNA decay. *Biochim Biophys Acta*. 2013; 1829: 695–707. doi: [10.1016/j.bbagr.2013.01.001](#) PMID: [23328451](#)
12. Timchenko NA, Patel R, Iakova P, Cai Z-J, Quan L, Timchenko LT. Overexpression of CUG triplet repeat-binding protein, CUGBP1, in mice inhibits myogenesis. *J Biol Chem*. 2004; 279: 13129–13139. doi: [10.1074/jbc.M312923200](#) PMID: [14722059](#)
13. Ward AJ, Rimer M, Killian JM, Dowling JJ, Cooper TA. CUGBP1 overexpression in mouse skeletal muscle reproduces features of myotonic dystrophy type 1. *Hum Mol Genet*. 2010; 19: 3614–3622. doi: [10.1093/hmg/ddq277](#) PMID: [20603324](#)
14. Timchenko LT, Miller JW, Timchenko NA, DeVore DR, Datar KV, Lin L, et al. Identification of a (CUG)_n triplet repeat RNA-binding protein and its expression in myotonic dystrophy. *Nucleic Acids Res*. 1996; 24: 4407–4414. PMID: [8948631](#)
15. Corbeil-Girard L-P, Klein AF, Sasseville AM-J, Lavoie H, Dicaire M-J, Saint-Denis A, et al. PABPN1 overexpression leads to upregulation of genes encoding nuclear proteins that are sequestered in oculopharyngeal muscular dystrophy nuclear inclusions. *Neurobiol Dis*. 2005; 18: 551–567. doi: [10.1016/j.nbd.2004.10.019](#) PMID: [15755682](#)
16. Sofola OA, Jin P, Qin Y, Duan R, Liu H, de Haro M, et al. RNA-binding proteins hnRNP A2/B1 and CUGBP1 suppress fragile X CGG premutation repeat-induced neurodegeneration in a Drosophila model of FXTAS. *Neuron*. 2007; 55: 565–571. doi: [10.1016/j.neuron.2007.07.021](#) PMID: [17698010](#)
17. Kuyumcu-Martinez NM, Wang G-S, Cooper TA. Increased steady-state levels of CUGBP1 in myotonic dystrophy 1 are due to PKC-mediated hyperphosphorylation. *Mol Cell*. 2007; 28: 68–78. doi: [10.1016/j.molcel.2007.07.027](#) PMID: [17936705](#)
18. Ohsawa N, Koebis M, Mitsuhashi H, Nishino I, Ishiura S. ABLIM1 splicing is abnormal in skeletal muscle of patients with DM1 and regulated by MBNL, CELF and PTBP1. *Genes Cells* 2015; 20: 121–134. doi: [10.1111/gtc.12201](#) PMID: [25403273](#)
19. Ho TH, Bundman D, Armstrong DL, Cooper TA. Transgenic mice expressing CUG-BP1 reproduce splicing mis-regulation observed in myotonic dystrophy. *Hum Mol Genet*. 2005; 14: 1539–1547. doi: [10.1093/hmg/ddi162](#) PMID: [15843400](#)
20. Philips AV, Timchenko LT, Cooper TA. Disruption of splicing regulated by a CUG-binding protein in myotonic dystrophy. *Science*. 1998; 280: 737–741. PMID: [9563950](#)

21. Paul S, Dansithong W, Kim D, Rossi J, Webster NJG, Comai L, et al. Interaction of muscleblind, CUG-BP1 and hnRNP H proteins in DM1-associated aberrant IR splicing. *EMBO J*. 2006; 25: 4271–4283. doi: [10.1038/sj.emboj.7601296](https://doi.org/10.1038/sj.emboj.7601296) PMID: [16946708](https://pubmed.ncbi.nlm.nih.gov/16946708/)
22. Akopian D, Shen K, Zhang X, Shan S. Signal Recognition Particle: An essential protein targeting machine. *Annu Rev Biochem*. 2013; 82: 693–721. doi: [10.1146/annurev-biochem-072711-164732](https://doi.org/10.1146/annurev-biochem-072711-164732) PMID: [23414305](https://pubmed.ncbi.nlm.nih.gov/23414305/)
23. Politz JC, Yarovoi S, Kilroy SM, Gowda K, Zwieb C, Pederson T. Signal recognition particle components in the nucleolus. *Proc Natl Acad Sci U S A*. 2000; 97: 55–60. PMID: [10618370](https://pubmed.ncbi.nlm.nih.gov/10618370/)
24. Wild K, Sinning I. RNA gymnastics in mammalian signal recognition particle assembly. *RNA Biol*. 2015; 11: 1330–1334.
25. Zhang X, Shan S. Fidelity of cotranslational protein targeting by the signal recognition particle. *Annu Rev Biophys*. 2014; 43: 381–408. doi: [10.1146/annurev-biophys-051013-022653](https://doi.org/10.1146/annurev-biophys-051013-022653) PMID: [24895856](https://pubmed.ncbi.nlm.nih.gov/24895856/)
26. Rahimov F, Kunkel LM. Cellular and molecular mechanisms underlying muscular dystrophy. *J Cell Biol*. 2013; 201: 499–510. doi: [10.1083/jcb.201212142](https://doi.org/10.1083/jcb.201212142) PMID: [23671309](https://pubmed.ncbi.nlm.nih.gov/23671309/)
27. Ghirardello A, Bassi N, Palma L, Borella E, Domeneghetti M, Punzi L, et al. Autoantibodies in polymyositis and dermatomyositis. *Curr Rheumatol Rep*. 2013; 15: 335. doi: [10.1007/s11926-013-0335-1](https://doi.org/10.1007/s11926-013-0335-1) PMID: [23591825](https://pubmed.ncbi.nlm.nih.gov/23591825/)
28. Benveniste O, Romero NB. Myositis or dystrophy? Traps and pitfalls. *Presse Médicale*. 2011; 40: e249–e255.
29. Stewart SA, Dykxhoorn DM, Palliser D, Mizuno H, Yu EY, An DS, et al. Lentivirus-delivered stable gene silencing by RNAi in primary cells. *RNA*. 2003; 9: 493–501. doi: [10.1261/rna.2192803](https://doi.org/10.1261/rna.2192803) PMID: [12649500](https://pubmed.ncbi.nlm.nih.gov/12649500/)
30. Moraes KCM, Wilusz CJ, Wilusz J. CUG-BP binds to RNA substrates and recruits PARN deadenylase. *RNA*. 2006; 12: 1084–1091. doi: [10.1261/rna.59606](https://doi.org/10.1261/rna.59606) PMID: [16601207](https://pubmed.ncbi.nlm.nih.gov/16601207/)
31. Zhang L, Lee JE, Wilusz J, Wilusz CJ. The RNA-binding protein CUGBP1 regulates stability of tumor necrosis factor mRNA in muscle cells: implications for myotonic dystrophy. *J Biol Chem*. 2008; 283: 22457–22463. doi: [10.1074/jbc.M802803200](https://doi.org/10.1074/jbc.M802803200) PMID: [18559347](https://pubmed.ncbi.nlm.nih.gov/18559347/)
32. Niranjankumari S, Lasda E, Brazas R, Garcia-Blanco MA. Reversible cross-linking combined with immunoprecipitation to study RNA-protein interactions in vivo. *Methods* 2002; 26: 182–190. doi: [10.1016/S1046-2023\(02\)00021-X](https://doi.org/10.1016/S1046-2023(02)00021-X) PMID: [12054895](https://pubmed.ncbi.nlm.nih.gov/12054895/)
33. Badr CE, Hewett JW, Breakefield XO, Tannous BA. A highly sensitive assay for monitoring the secretory pathway and ER stress. *PLoS One*. 2007; 2: e571. doi: [10.1371/journal.pone.0000571](https://doi.org/10.1371/journal.pone.0000571) PMID: [17593970](https://pubmed.ncbi.nlm.nih.gov/17593970/)
34. Rädle B, Rutkowski AJ, Ruzsics Z, Friedel CC, Koszinowski UH, Dölken L. Metabolic labeling of newly transcribed RNA for high resolution gene expression profiling of RNA synthesis, processing and decay in cell culture. *J Vis Exp*. 2013;
35. Duffy EE, Rutenberg-Schoenberg M, Stark CD, Kitchen RR, Gerstein MB, Simon MD. Tracking Distinct RNA Populations Using Efficient and Reversible Covalent Chemistry. *Mol Cell*. 2015; 59: 858–866. doi: [10.1016/j.molcel.2015.07.023](https://doi.org/10.1016/j.molcel.2015.07.023) PMID: [26340425](https://pubmed.ncbi.nlm.nih.gov/26340425/)
36. Miller C, Schwalb B, Maier K, Schulz D, Dümcke S, Zacher B, et al. Dynamic transcriptome analysis measures rates of mRNA synthesis and decay in yeast. *Mol Syst Biol*. 2011; 7: 458. doi: [10.1038/msb.2010.112](https://doi.org/10.1038/msb.2010.112) PMID: [21206491](https://pubmed.ncbi.nlm.nih.gov/21206491/)
37. Lee JE, Lee JY, Trembly J, Wilusz J, Tian B, Wilusz CJ. The PARN deadenylase targets a discrete set of mRNAs for decay and regulates cell motility in mouse myoblasts. *PLoS Genet*. 2012; 8: e1002901. doi: [10.1371/journal.pgen.1002901](https://doi.org/10.1371/journal.pgen.1002901) PMID: [22956911](https://pubmed.ncbi.nlm.nih.gov/22956911/)
38. Rattenbacher B, Beisang D, Wiesner DL, Jeschke JC, von Hohenberg M, St Louis-Vlasova IA, et al. Analysis of CUGBP1 targets identifies GU-repeat sequences that mediate rapid mRNA decay. *Mol Cell Biol*. 2010; 30: 3970–3980. doi: [10.1128/MCB.00624-10](https://doi.org/10.1128/MCB.00624-10) PMID: [20547756](https://pubmed.ncbi.nlm.nih.gov/20547756/)
39. Beisang D, Reilly C, Bohjanen PR. Alternative polyadenylation regulates CELF1/CUGBP1 target transcripts following T cell activation. *Gene*. 2014; 550: 93–100. doi: [10.1016/j.gene.2014.08.021](https://doi.org/10.1016/j.gene.2014.08.021) PMID: [25123787](https://pubmed.ncbi.nlm.nih.gov/25123787/)
40. Yu T-X, Rao JN, Zou T, Liu L, Xiao L, Ouyang M, et al. Competitive binding of CUGBP1 and HuR to occludin mRNA controls its translation and modulates epithelial barrier function. *Mol Biol Cell*. 2013; 24: 85–99. doi: [10.1091/mbc.E12-07-0531](https://doi.org/10.1091/mbc.E12-07-0531) PMID: [23155001](https://pubmed.ncbi.nlm.nih.gov/23155001/)
41. Liu L, Ouyang M, Rao JN, Zou T, Xiao L, Chung HK, et al. Competition between RNA-binding proteins CELF1 and HuR modulates MYC translation and intestinal epithelium renewal. *Mol Biol Cell*. 2015; 26: 1797–1810. doi: [10.1091/mbc.E14-11-1500](https://doi.org/10.1091/mbc.E14-11-1500) PMID: [25808495](https://pubmed.ncbi.nlm.nih.gov/25808495/)
42. Bauermeister D, Claußen M, Pieler T. A novel role for Celf1 in vegetal RNA localization during *Xenopus* oogenesis. *Dev Biol*. 2015; 405: 214–224. doi: [10.1016/j.ydbio.2015.07.005](https://doi.org/10.1016/j.ydbio.2015.07.005) PMID: [26164657](https://pubmed.ncbi.nlm.nih.gov/26164657/)

43. Roots R, Smith KC. Effects of actinomycin D on cell cycle kinetics and the DNA of Chinese hamster and mouse mammary tumor cells cultivated in vitro. *Cancer Res.* 1976; 36: 3654–3658. PMID: [986240](#)
44. Sawicki SG, Godman GC. On the differential cytotoxicity of actinomycin D. *J Cell Biol.* 1971; 50: 746–761. PMID: [4398631](#)
45. Harrold S, Genovese C, Kobrin B, Morrison SL, Milcarek C. A comparison of apparent mRNA half-life using kinetic labeling techniques vs decay following administration of transcriptional inhibitors. *Anal Biochem.* 1991; 198: 19–29. PMID: [1789423](#)
46. Seiser C, Posch M, Thompson N, Kühn LC. Effect of transcription inhibitors on the iron-dependent degradation of transferrin receptor mRNA. *J Biol Chem.* 1995; 270: 29400–29406. PMID: [7493976](#)
47. Friedel CC, Dölken L, Ruzsics Z, Koszinowski UH, Zimmer R. Conserved principles of mammalian transcriptional regulation revealed by RNA half-life. *Nucleic Acids Res.* 2009; 37: e115. doi: [10.1093/nar/gkp542](#) PMID: [19561200](#)
48. Maekawa S, Imamachi N, Irie T, Tani H, Matsumoto K, Mizutani R, et al. Analysis of RNA decay factor mediated RNA stability contributions on RNA abundance. *BMC Genomics.* 2015;16.
49. Dori-Bachash M, Shalem O, Manor YS, Pilpel Y, Tirosh I. Widespread promoter-mediated coordination of transcription and mRNA degradation. *Genome Biol.* 2012; 13: R114. doi: [10.1186/gb-2012-13-12-r114](#) PMID: [23237624](#)
50. Sun M, Schwalb B, Schulz D, Pirkl N, Etzold S, Larivière L, et al. Comparative dynamic transcriptome analysis (cDTA) reveals mutual feedback between mRNA synthesis and degradation. *Genome Res.* 2012;
51. Shalem O, Groisman B, Choder M, Dahan O, Pilpel Y. Transcriptome kinetics is governed by a genome-wide coupling of mRNA production and degradation: a role for RNA Pol II. *PLoS Genet.* 2011; 7: e1002273. doi: [10.1371/journal.pgen.1002273](#) PMID: [21931566](#)
52. Sun M, Schwalb B, Pirkl N, Maier KC, Schenk A, Failmezger H, et al. Global analysis of eukaryotic mRNA degradation reveals Xrn1-dependent buffering of transcript levels. *Mol Cell.* 2013; 52: 52–62. doi: [10.1016/j.molcel.2013.09.010](#) PMID: [24119399](#)
53. Unlu G, Levic DS, Melville DB, Knapik EW. Trafficking mechanisms of extracellular matrix macromolecules: Insights from vertebrate development and human diseases. *Int J Biochem Cell Biol.* 2014; 47: 57–67. doi: [10.1016/j.biocel.2013.11.005](#) PMID: [24333299](#)
54. Charras G, Sahai E. Physical influences of the extracellular environment on cell migration. *Nat Rev Mol Cell Biol.* 2014; 15: 813–824. doi: [10.1038/nrm3897](#) PMID: [25355506](#)
55. Deshmukh AS, Murgia M, Nagaraj N, Treebak JT, Cox J, Mann M. Deep proteomics of mouse skeletal muscle enables quantitation of protein isoforms, metabolic pathways, and transcription factors. *Mol Cell Proteomics.* 2015; 14: 841–853. doi: [10.1074/mcp.M114.044222](#) PMID: [25616865](#)
56. Bovia F, Fornallaz M, Leffers H, Strub K. The SRP9/14 subunit of the signal recognition particle (SRP) is present in more than 20-fold excess over SRP in primate cells and exists primarily free but also in complex with small cytoplasmic Alu RNAs. *Mol Biol Cell.* 1995; 6: 471–484. PMID: [7542942](#)
57. Ren Y-F, Li G, Wu J, Xue Y-F, Song Y-J, Lv L, et al. Dicer-dependent biogenesis of small RNAs derived from 7SL RNA. *PloS One.* 2012; 7: e40705. doi: [10.1371/journal.pone.0040705](#) PMID: [22808238](#)
58. Ren Y-F, Li G, Xue Y-F, Zhang X-J, Song Y-J, Lv L, et al. Decreased dicer expression enhances SRP-mediated protein targeting. *PloS One.* 2013; 8: e56950. doi: [10.1371/journal.pone.0056950](#) PMID: [23468895](#)
59. Beisang D, Rattenbacher B, Vlasova-St Louis IA, Bohjanen PR. Regulation of CUG-binding protein 1 (CUGBP1) binding to target transcripts upon T cell activation. *J Biol Chem.* 2012; 287: 950–960. doi: [10.1074/jbc.M111.291658](#) PMID: [22117072](#)
60. Palumbo MC, Farina L, Paci P. Kinetics effects and modeling of mRNA turnover. *Wiley Interdiscip Rev RNA.* 2015; 6: 327–336. doi: [10.1002/wrna.1277](#) PMID: [25727049](#)